

28). Interestingly, a recent theoretical study on the HF dissociation-recombination reaction (29) has led to a conclusion in favor of a three-stage proton-transfer reaction mechanism and has found a concerted reaction mechanism upon diffusional encounter to be energetically unfavored.

#### References and Notes

- P. L. Geissler, C. Dellago, D. Chandler, J. Hutter, M. Parrinello, *Science* **291**, 2121 (2001).
- D. Marx, M. E. Tuckerman, J. Hutter, M. Parrinello, *Nature* **397**, 601 (1999).
- R. P. Bell, *The Proton in Chemistry* (Chapman and Hall, London, ed. 2, 1973).
- D. N. Silverman, *Biochim. Biophys. Acta* **1458**, 88 (2000).
- W. Kühnbrandt, *Nature* **406**, 569 (2000), and references therein.
- M. Eigen, W. Kruse, L. De Maeyer, *Progr. React. Kinet.* **2**, 285 (1964).
- M. Eigen, *Angew. Chem. Int. Ed.* **3**, 1 (1964).
- A. Weller, *Progr. React. Kinet.* **1**, 187 (1961).
- J. L. Skinner, H. P. Trommsdorff, *J. Chem. Phys.* **89**, 897 (1988).
- A. J. Leggett *et al.*, *Rev. Mod. Phys.* **59**, 1 (1987).
- P. Hänggi, P. Talkner, M. Borkovec, *Rev. Mod. Phys.* **62**, 251 (1990).
- A. Oppenländer, C. Rambaud, H. P. Trommsdorff, J.-C. Vial, *Phys. Rev. Lett.* **63**, 1432 (1989).
- K. Ando, J. T. Hynes, *Adv. Chem. Phys.* **110**, 381 (1999).
- T. Elsaesser, in *Ultrafast Hydrogen Bonding and Proton Transfer Processes in the Condensed Phase*, T. Elsaesser, H. J. Bakker, Eds. (Kluwer, Dordrecht, Netherlands, 2002), pp. 119–153.
- L. M. Tolbert, K. M. Soltsev, *Acc. Chem. Res.* **35**, 1 (2002).
- E. Pines, D. Pines, in *Ultrafast Hydrogen Bonding and Proton Transfer Processes in the Condensed Phase*, T. Elsaesser, H. J. Bakker, Eds. (Kluwer, Dordrecht, Netherlands, 2002), pp. 155–184.
- A. Douhal, S. K. Kim, A. H. Zewail, *Nature* **378**, 260 (1995).
- Practical experimental issues concern limited time resolution in time-correlated single-photon counting and excited-state absorption in pump-probe spectroscopy.
- E. Pines, D. Huppert, N. Agmon, *J. Chem. Phys.* **88**, 5620 (1988).
- E. Pines, B.-Z. Magnes, M. J. Lang, G. R. Fleming, *Chem. Phys. Lett.* **281**, 413 (1997).
- L. T. Genosar, B. Cohen, D. Huppert, *J. Phys. Chem. A* **104**, 6689 (2000).
- T.-H. Tran-Thi, T. Gustavsson, C. Prayer, S. Pommeret, J. T. Hynes, *Chem. Phys. Lett.* **329**, 421 (2000).
- Bands between 950 and 1250  $\text{cm}^{-1}$  are associated with motions of the  $\text{SO}_3^-$  groups and do not show large changes upon proton transfer of HPTS.
- Details of the experimental methods and modeling can be found at *Science* Online.
- The 1539  $\text{cm}^{-1}$  band of the photoacid and the photobase band at 1503  $\text{cm}^{-1}$  cannot be detected in the case of high acetate concentrations because of a nearby acetate band.
- This same value is obtained by analyzing solvatochromic shifts of the electronic absorption bands of HPTS as function of acetate concentration.
- A. Szabo, *J. Phys. Chem.* **93**, 6929 (1989).
- W. C. Natzle, C. B. Moore, *J. Phys. Chem.* **89**, 2605 (1985).
- K. Ando, J. T. Hynes, *J. Phys. Chem. A* **103**, 10398 (1999).
- G. Zundel, *Adv. Chem. Phys.* **111**, 1 (2000).
- The progress has benefited from the financial support of the Deutsche Forschungsgemeinschaft (Project DFG NI 492/2-2) and the German-Israeli Foundation for Scientific Research and Development (Project GIF 722/01) and from comments by C. Lienau and H. Fidder; B.Z.M. acknowledges financial travel support through the LIMANS Cluster of Large Scale Laser Facilities (Project MBI000228).

#### Supporting Online Material

www.sciencemag.org/cgi/content/full/301/5631/349/DC1  
Materials and Methods  
SOM Text  
16 April 2003; accepted 4 June 2003

## Programmed Adsorption and Release of Proteins in a Microfluidic Device

Dale L. Huber, Ronald P. Manginell, Michael A. Samara, Byung-Il Kim, Bruce C. Bunker\*

A microfluidic device has been developed that can adsorb proteins from solution, hold them with negligible denaturation, and release them on command. The active element in the device is a 4-nanometer-thick polymer film that can be thermally switched between an antifouling hydrophilic state and a protein-adsorbing state that is more hydrophobic. This active polymer has been integrated into a microfluidic hot plate that can be programmed to adsorb and desorb protein monolayers in less than 1 second. The rapid response characteristics of the device can be manipulated for proteomic functions, including preconcentration and separation of soluble proteins on an integrated fluidics chip.

Microfluidic systems are being developed that can separate, purify, analyze, and deliver biomolecules (1–3), but, as system dimensions become smaller, interfacial interactions begin to dominate device performance. For example, adsorption of proteins onto surfaces can result in fouling, the denaturing of the proteins, and consumption of precious samples. Interfacial interactions are often manipulated with self-assembled monolayers (SAMs). Although globular proteins tend to adsorb on hydrocarbon-terminated SAMs, termination with polyethylene oxide (PEO) results in an antifouling surface (4–6).

Passive SAMs are widely used in microfluidics, but it is becoming clear (7, 8) that greater functionality can be provided in more sophisticated separations and sensor systems with the use of active coatings that can change their surface chemistry in response to on-chip stimuli such as applied voltages, heat, or light. With active coatings, the surface can be programmed to adsorb or release proteins for applications such as protein preconcentrators for on-chip two-dimensional protein separations. We describe a device in which reversible protein adsorption has been demonstrated with the use of thermal activation of a polymeric film.

The active material in this switchable protein trap is an end-tethered monolayer of poly(*N*-isopropylacrylamide) (PNIPAM). This polymer exhibits a lower critical solution temperature (LCST), a temperature above which the polymer becomes insoluble, in water at about 35°C (9–11). At room temperature, the polymer swells in water to create a relatively hydrophilic surface with a water contact angle that can be as low as 30°. Above the transition temperature, the water is expelled, the polymer collapses, and the surface becomes less hydrophilic, with a

water contact angle that can approach 90° (Fig. 1A). PNIPAM-functionalized particles and bulk hydrogels interact more strongly with proteins above the LCST (12, 13). At room temperature, the adsorption of large globular proteins such as human serum albumin (HSA) is negligible on a tethered PNIPAM film (Fig. 1B) and is comparable to that on PEO SAMs. Above the LCST, HSA adsorption is extensive. Complete protein monolayers form at rates comparable to those seen on hydrocarbon-terminated octadecyltrichlorosilane (ODTS) surfaces. For large globular proteins such as HSA, complete desorption is normally observed on cooling the PNIPAM films to room temperature.

In order for a film to be usable in a reversible protein trap for microfluidics, at least three requirements must be met: (i) the polymer needs to be in a configuration that supports the desired thermally activated phase transition, (ii) films must be robust and strongly attached to the surface, and (iii) protein adsorption must be reversible and rapid. The first two requirements are met by synthesis routes involving chain-grafting (10) or the in situ free radical polymerization of NIPAM on functionalized SAMs (14, 15). For in situ polymerization, the SAM chains are covalently bound to oxide-terminated surfaces with the use of silane coupling agents, satisfying the need for strong, robust surface attachment. The SAM chains are terminated with functionalities that generate free radicals at chain ends, stimulating the growth of polymer molecules covalently linked to the SAM. Unfortunately, our results indicate that, even when such films support reversible swelling transitions, reversible protein adsorption is often not observed. For example, films we have produced with the use of the tethered azo-radical initiator azobis(isobutyronitrile) (AIBN) (14) typically have high single-chain molecular weights [weight-average molecular weight ( $M_w$ ) around  $10^7$ ] and low grafting densities (on the order of  $2.5 \times 10^{10}$  chains/cm<sup>2</sup>, or a chain-chain separation of 60 to 70 nm). With such films, we find

Sandia National Laboratory, Post Office Box 5800, Albuquerque, NM 87185–1413, USA.

\*To whom correspondence should be addressed. E-mail: bcbunke@sandia.gov

that small gaps open up between chains upon collapse above the transition temperature, leading to irreversible adsorption of smaller proteins such as myoglobin (14).

We have been able to eliminate this irreversible adsorption by increasing the graft density of the polymer chains via an alternative chain-transfer reaction on SAM chains terminated with thiol groups. Here, free radicals are produced in solution with the use of thermal activation of AIBN and are transferred to tethered

thiols (16). In contrast to a conventional polymerization process, where chain transfer between surface-bound initiators yields a radical and a dead initiator, chain transfer between thiol groups exchanges a radical for a hydrogen atom, yielding a radical and a regenerated thiol. The result of fewer deleterious side reactions is higher grafting densities ( $10^{11}$  to  $10^{13}$  chains/cm<sup>2</sup>, or chains separated by 2 to 20 nm).

All of the tethered PNIPAM films discussed here exhibit a swelling transition similar to that

exhibited by bulk gels. This transition, and its impact on phenomena such as protein adsorption, can be visualized with an interfacial force microscope (IFM) (17). This scanning probe system enables us to monitor attractive and repulsive interactions between functionalized probe tips and PNIPAM-coated surfaces as a function of separation distance in water, avoiding the “snap-to-contact” problems associated with making such measurements with the use of an atomic force microscope (AFM). At room temperature, PNIPAM films generate a repulsive force on both approach and retraction of the tip regardless of tip coating. For films with high grafting densities (Fig. 2), this repulsion becomes apparent at a distance of around 100 nm above the glass substrate. On the azo-initiated film with a  $M_w$  of  $10^7$ , the repulsion is detected at 320 nm, which corresponds well to the hydrodynamic diameter of single chains (18). Above the LCST, the repulsive region collapses by about a factor of 2. We believe that the observed repulsion is because of physical contact between the tip and hydrated PNIPAM chains and that the collapse of the repulsive force reflects the collapse of the PNIPAM film above the LCST, consistent with reported AFM measurements (19). When the tip is retracted from the surface at temperatures above the LCST, the plot has an attractive well (the measured force drops below zero) that reflects adhesion between the PNIPAM and the tip. This reversible switching between repulsive and adhesive states below and above the LCST is consistent with the observed switching in protein adsorption behavior.

To be useful in microfluidics, responsive PNIPAM films need to be incorporated into a device in which rapid and controlled heating and cooling can be achieved in small volumes. Several research groups have demonstrated that resistive heater lines on silicon chips can be used to provide localized temperature control in fluidic systems for applications such as the thermally activated pumping of fluids (20). The system we have developed for studying PNIPAM is a micro-hot plate device (Fig.

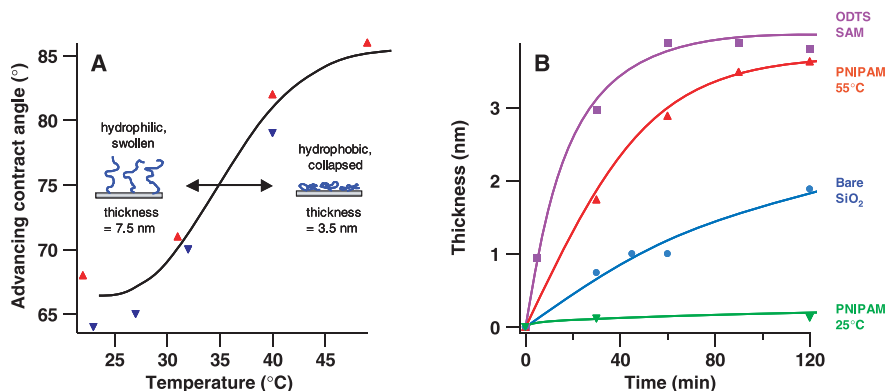


**Fig. 1.** (A) Water contact angle measurements obtained on an azo-initiated PNIPAM film as a function of temperature. Cartoons indicate the corresponding state (swollen or collapsed) of the film versus temperature. Although gels can exhibit contact angle changes as high as 60°, changes of 20° to 25° are more common on monolayer films. (B) Ellipsometry results showing the adsorption of HSA from a 0.5 mg/ml solution (0.05 M, pH = 6 phosphate buffer) on PNIPAM-coated surfaces relative to other model surfaces. Adsorption is negligible on PNIPAM below the transition temperature, whereas a protein monolayer eventually forms on PNIPAM above the transition temperature.

**Fig. 2.** IFM results obtained in deionized water between a hydrophobically modified glass tip (ODTS-coated) and a tethered PNIPAM film having a high grafting density. (A) Normal force profiles obtained on approach of the tip to the surface show a repulsive force that collapses into the surface above the PNIPAM transition temperature (~26°C for the example shown). (B) Normal force profiles obtained on retraction of the tip show strong adhesive interactions above the PNIPAM transition temperature (note 48°C curve).

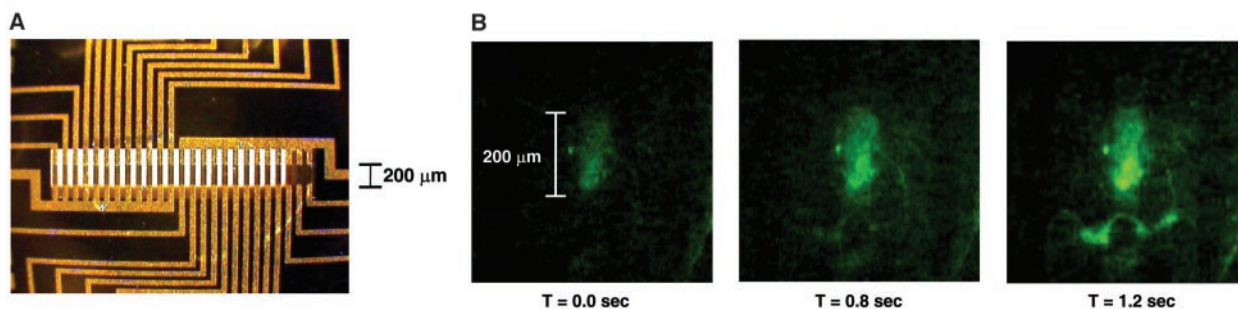
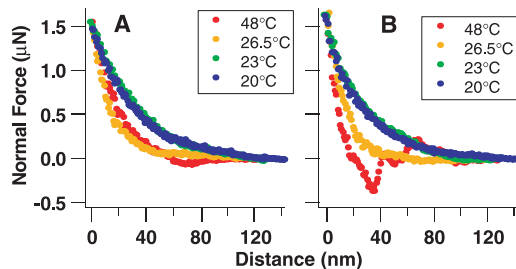


**Fig. 3.** (A) A photomicrograph of the hot plate showing the array of gold heater lines on top of a 200- $\mu$ m-wide  $\text{Si}_3\text{N}_4$  membrane (central white region). (B) Fluorescence microscopy images of fluorescein-labeled myoglobin (green) interacting with a single heated line. (Left) Image obtained on heating a line above the PNIPAM transition

temperature after exposure to a 0.5 mg/ml myoglobin solution followed by a rinse in myoglobin-free buffer. (Center and Right) Images were obtained 0.8 and 1.2 s after the hot line was turned off, releasing a plume of protein into a stagnant solution. Stills have been extracted from movie S1.

## REPORTS

3A) that consists of an array of gold or platinum heater lines deposited on a thin, freestanding layer of silicon nitride suspended over a silicon frame. A fluid volume of 3  $\mu\text{l}$  is confined over a working area of 2500  $\mu\text{m}$  by 200  $\mu\text{m}$ , with individual heater lines being 10, 20, or 50  $\mu\text{m}$  wide.

Protein trapping is achieved by heating individual lines above the LCST of 35°C. Gradients of 0.50°C/ $\mu\text{m}$  can be achieved, permitting close placement of separately controlled heater lines. In the device shown, heating is rapid (a line can be heated above the transition temperature in <1 ms). Given typical concentrations, diffusion coefficients (around  $10^{-6}$   $\text{cm}^2/\text{s}$ ), and sticking probabilities for proteins, the temperature response of the device is orders of magnitude faster than the kinetics of monolayer formation. Cooling is passive, but thermal equilibration is still rapid, requiring <1 s. The temperature can be controlled to within about 2°C, which is important to avoid overheating protein and causing denaturation.

The response characteristics of the fluidics device containing PNIPAM films have been tested by monitoring the adsorption and desorption of fluorescein-labeled myoglobin from static solutions with the use of fluorescence microscopy. For example, one line in the heater array has been taken above the LCST while in contact with a 0.5 mg/ml solution of labeled myoglobin in 0.01 M phosphate buffer (pH = 6.5). The active region is then flushed with a myoglobin-free buffer solution to remove all unadsorbed protein. Fluorescence microscopy reveals a layer of myoglobin forms only on the PNIPAM above the heated line (Fig. 3B and movie S1). An image taken less than 1 s after the heater line is turned off shows a convectively driven plume of fluorescent myoglobin desorbing from the surface (Fig. 3B). The fluorescence intensity in the plume is higher than the intensity of the initial protein film because the fluorophores in solution

do not quench each other as they do in their highly packed state in the monolayer. For myoglobin, the desorption process is complete in <2 s. Although fluorescence microscopy results on single heater lines demonstrate that localized, rapid adsorption and subsequent desorption are achievable within the hot plate device, these results are qualitative.

A number of more quantitative measurements have been taken on extended surfaces with ultraviolet (UV)-visible spectroscopy to demonstrate the competitive adsorption kinetics needed for separations. Mixtures of myoglobin and bovine serum albumin (BSA), hemoglobin and BSA, and cytochrome C and BSA were exposed to PNIPAM films above the LCST. (Myoglobin, hemoglobin, and cytochrome C all contain heme groups as a native chromophore, and the BSA was tagged with fluorescein.) For solutions containing myoglobin and tagged BSA (Fig. 4A), the smaller myoglobin ( $M_w$  of 16,000) is adsorbed almost immediately, forming a monolayer within tens of seconds. The spectra suggest that the layer is 95% dense after 30 s, containing 75% and 20% of myoglobin and albumin, respectively. However, within minutes, the larger BSA ( $M_w$  of 65,000) displaces the myoglobin to form a relatively pure BSA monolayer. The composition of the initial monolayer depends on relative protein concentrations as well as the nature of the competing proteins. For example, 30% more BSA is present in the initial film if the myoglobin:BSA ratio in solution is increased from 1:4 to 1:16. Whereas cytochrome C, the smallest protein investigated, forms relatively pure monolayers at short times (Fig. 4B), hemoglobin, having a molecular weight ( $M_w$  of 64,500) comparable to that of albumin, is only slightly more competitive than albumin in the initial adsorption stage (Fig. 4C). However, even hemoglobin is displaced by albumin within a few minutes. These results are consistent with literature studies of competitive

protein adsorption on passive surfaces (21). A simple analysis indicates that the initial adsorption is dominated by kinetics (protein diffusion is inversely proportional to the hydrodynamic radius) (22) but that the final make-up of the protein layer is related to thermodynamics (larger proteins tend to adsorb more strongly because they interact over a larger contact area.)

The competitive adsorption results suggest how the protein trap could be used for programmable protein separations. For the myoglobin-BSA example shown, the protein trap could selectively adsorb either myoglobin or BSA from myoglobin-BSA mixtures depending on fluid residence and hot line activation times. Proteins could be trapped at specific locations from a dilute feed, and, once concentrated, released into individual on-chip separation columns. Arrays of such devices could be used to rapidly optimize the conditions needed to extract particular proteins of interest on a larger scale. The protein trap may also be useful for creating highly selective bioassays. We are currently investigating the use of the trap to create and regenerate highly selective antibody monolayers.

### References and Notes

- G. M. Whitesides, A. D. Stroock, *Phys. Today* **54**, 42 (2001).
- D. Figeys, D. Pinto, *Electrophoresis* **22**, 208 (2001).
- J. C. McDonald *et al.*, *Electrophoresis* **21**, 27 (2000).
- P. Harder, M. Grunze, R. Dahint, G. M. Whitesides, P. E. Laibinis, *J. Phys. Chem. B* **102**, 426 (1998).
- E. Ostuni, L. Yan, G. M. Whitesides, *Colloids Surf. B* **15**, 3 (1999).
- K. L. Prime, G. M. Whitesides, *Science* **252**, 1164 (1991).
- N. Abbott, C. Gorman, G. Whitesides, *Langmuir* **11**, 16 (1995).
- J. Lahann *et al.*, *Science* **299**, 371 (2003).
- R. Pelton, *Adv. Colloid Interface Sci.* **85**, 1 (2000).
- Y. G. Takei *et al.*, *Macromolecules* **27**, 6163 (1994).
- J. Zhang, R. Pelton, Y. Deng, *Langmuir* **11**, 2301 (1995).
- H. Lakhari *et al.*, *Biochim. Biophys. Acta* **1379**, 303 (1998).
- H. Kanazawa *et al.*, *Anal. Chem.* **68**, 100 (1996).
- Details of the synthetic procedures, UV-visible spectroscopy studies, and microfluidics are available on Science Online.
- L. Liang, X. D. Feng, J. Liu, P. C. Rieke, G. E. Fryxell, *Macromolecules* **31**, 7845 (1998).
- A. Revillon, D. Leroux, *React. Funct. Polym.* **26**, 105 (1995).
- S. A. Joyce, J. E. Houston, *Rev. Sci. Instrum.* **62**, 710 (1991).
- C. Wu, S. Zhou, *Macromolecules* **28**, 8381 (1995).
- S. Kidoaki, S. Ohya, Y. Nakayama, T. Matsuda, *Langmuir* **17**, 2402 (2001).
- M. Burns *et al.*, *Proc. Natl. Acad. Sci. U.S.A.* **93**, 5556 (1996).
- M. Kleijn, W. Norde, *Heterogeneous Chem. Rev.* **2**, 157 (1995).
- B. J. Berne, R. Pecora, *Dynamic Light Scattering* (Dover, Mineola, NY, 2000).
- Supported by the Division of Materials Science and Engineering, Office of Basic Energy Sciences, U.S. Department of Energy (DOE), and by Laboratory Directed Research and Development funds at Sandia National Laboratories. Sandia is a multiprogram laboratory operated by Sandia Corporation, a Lockheed Martin company, for DOE under contract DE-ACO4-94AL8500.

**Supporting Online Material**  
www.sciencemag.org/cgi/content/full/301/5631/352/DC1  
Materials and Methods  
Figs. S1 to S4  
Movie S1

22 November 2002; accepted 12 June 2003

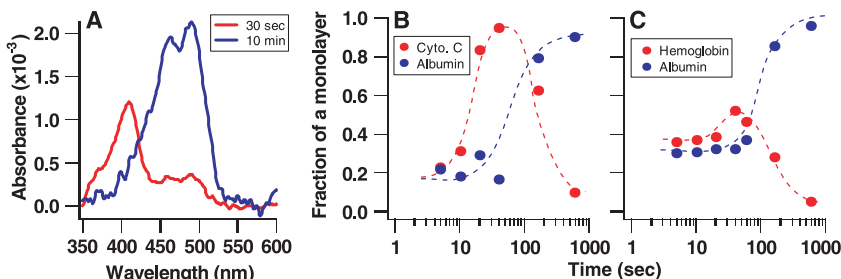


**Fig. 4.** Competitive adsorption of proteins on PNIPAM brush films immersed in 50°C protein solutions (1:4 mixtures of the indicated protein to BSA, total protein concentration = 0.5 mg/ml) as monitored with the use of UV-visible spectroscopy. For (B) and (C), lines are provided to guide the eye. (A) UV-visible spectra obtained films immersed in 1:4 myoglobin:BSA as a function of immersion time. The myoglobin adsorption band at 408 nm constitutes a monolayer when the absorbance is  $1.6 \times 10^{-3}$ , whereas the bands for labeled albumin at 465 nm and 495 nm represent a monolayer when the maximum absorbance is  $2 \times 10^{-3}$ . (B) Fractions of protein monolayers adsorbed on PNIPAM brush films versus time for the cytochrome C-BSA mixture. (C) Fractions of protein monolayers adsorbed on PNIPAM brush films versus immersion time in hemoglobin-BSA solutions. Hemoglobin adsorption is less extensive than that of cytochrome C, both exhibit maximum surface concentrations in 30 to 40 s, and both are almost completely displaced by albumin in 10 minutes.